Plasma Chemistry and Plasma Processing, Vol. 25, No. 5, October 2005 (© 2005)
DOI: 10.1007/s11090-005-4994-1

Chemical and Transport Properties of Carbon–Oxygen–Hydrogen Plasmas in Isochoric Conditions

Bernard Pateyron,[1,2] Guy Delluc,[1] and Pierre Fauchais[1]

Received August 2, 2004; revised January 12, 2005

The composition and transport properties of CO_2, CO, CH_4, $CO + Ar$ (50 vol%), $CO + Fe$ (50 vol%) have been calculated at constant volume assuming local thermodynamic equilibrium (LTE). Except at low temperature ($T < 3000$ K), when the formation of condensed species or more complex molecules can occur, pressure increases with temperature at constant volume. For example, for 1 mol of CH_4 starting at 0.1 MPa and 298 K the pressure can reach 40 MPa at 20,000 K. The consequence is a shift to higher temperatures of dissociation and ionization. The electrical conductivity σ_e at constant volume increases drastically relative to that obtained at 0.1 MPa over 15,000 K, in spite of the decrease of the electron density n_e This is due to the increase in the neutral species density. n_i, with a much lower electron-neutral species collision cross section σ_{ei} (σ_e is inversely proportional to n_i, σ_{ei}). The viscosity always exhibits a maximum when the ionization degree increases over 1–30%, but this maximum is shifted to higher temperatures and its peak value is higher. The thermal conductivity peaks due to dissociation and ionization are shifted to higher temperatures and their values are reduced compared to those obtained at constant pressure.

KEY WORDS: Thermodynamic equilibrium; isochoric conditions; transport properties; gaseous mixture; carbon; oxygen; hydrogen.

Nomenclature

$B(T)$	second virial coefficient (m^{-3})
$C(T)$	third virial coefficient (m^{-6})
k	Boltzmann constant (1.38066×10^{-23} J/K particle)
K	thermal conductivity (W/m K)
M_i	mass of particle of species i (kg)
n'	total number of moles (mole)
n'_i	mole number of species i (-)

[1] SPCTS UMR CNRS 6638, 123, Avenue Albert Thomas, 87060 Limoges Cedex, France.
[2] To whom correspondence should be addressed. E-mail: bernard.pateyron@unilim.fr

n_i	density of species i (m^{-3})
Nav	Avogadro's number ($6.022045 \times 10^{+23}$ particles/mol)
p	pressure (Pa)
R	perfect gas constant (8.31451 J/K mole)
V	volume (m^3)
ε_n	depth of non-polar potential (J)
$\varepsilon_{n,p}$	empirical potential depth (J)
ε_p	depth of polar potential (J)
μ'	dipole momentum in Debyes (1 Debye $= 3.162 \times 10^{-25} (J\,m^3)^{1/2}$
μ	viscosity (kg/m s)
$\sigma_{i,j}$	collision cross section (hard spheres) between particle i and particle j (m^2)
σ_e	electrical conductivity (mho/m)
σ_n	non-polar width of the potential (m)
$\sigma_{n,p}$	empirical potential width (m)
σ_p	polar width of the potential (m)
$\overline{\Omega}_{i,j}^{l,s}$	dimensionless collision integral between particle i and particle j with the approximation coefficients l and s

1. INTRODUCTION

The production of ferroalloys is achieved mainly by submerged arc furnaces:[1,2] ferromanganese high grade 4.6 Mt/y and ferrochromium high carbon 3.1 Mt/y. In 1998, the annual electric power consumption in submerged arc furnaces worldwide represented 30–40 billions of kWh. Moreover, since the beginning of their development, about 10 years ago, 125 direct current (d.c.) arc furnaces with power levels between 70 and 100 MW have been built or were under construction worldwide by 1998.[1,2] Besides its advantages over alternating current (a.c.), d.c. results in longer arcs requiring a high foaming slag layer to trap the arc radiation. Thus in both types of arcs, reactions within the plasma are not isobaric over the length of the arc and there are uncertain or mixed conditions of state. Thus at some location the reaction can be considered as isochoric. All of the many calculations of plasma compositions and transport properties that have been done (see the review in Ref. 3) were performed at constant pressure and none, to our knowledge, at constant volume. Thus the aim of this paper is to underline the differences occurring when performing such calculations at constant volume. After briefly describing the calculations, the results obtained at equilibrium with CO or CO_2, CO and Ar, CH_4, CO and Fe will be presented and discussed.

2. CALCULATION OF THERMODYNAMIC AND TRANSPORT PROPERTIES AT EQUILIBRIUM

2.1. Thermodynamic Properties

The algorithm of the Gibbs free energy minimization at constant pressure, already described,[4] has been used. Solid or liquid species and their sublimation or decomposition can be taken into account. For example the formation and the sublimation of solid carbon C(s) is important for CH_4. Firstly for a given mixture (usually 1 mol) the constant volume is defined as that corresponding to 300 K and 10^5 Pa. Then a new volume is calculated for the temperature T. At the first iteration, the pressure is readjusted in such a way that the volume is kept constant and so on. It means that after n iterations the composition and pressure of the plasma are obtained for the chosen temperature and constant volume. If at low temperature ($T < 3000$ K) condensed species or more complex molecules (e.g. $2\ CO + O_2 \Rightarrow 2CO_2$) are formed the pressure can diminish when temperature increases. In all other cases, pressure increases with temperature. Thus in these calculations, the virial effect correction has been systematically taken in account, in spite of the fact that it only introduces small changes.

2.2. Virial Equation of State

The virial equation of state is generally written as:

$$\frac{pV}{n'RT} = 1 + \frac{B(T)}{V} + \frac{C(T)}{V^2} + \cdots,$$

where R is the perfect gas constant, T the temperature and n' the number of moles, p the pressure and V the volume occupied by the gas.

The coefficients $B(T)$, $C(T)$, ... are called the second, third ... virial coefficients. By means of statistical mechanics these virial coefficients may be expressed in terms of the intermolecular potential functions and represent the deviation from the ideal behavior when collisions involving successively two, three... molecules become important in the gas.

From Hirschfelder[5] $B(T)$ is expressed as:

$$B(T) = -\frac{2\pi N_{\text{av}}}{3kT} \int_0^\infty r^3 \frac{d\varphi}{dr} e^{-\varphi(r)/kT}\, dr, \tag{1}$$

where $\varphi(r)$ is the intermolecular potential function at the intermolecular distance r, k the Boltzmann constant, T the temperature and N_{av},

the Avogadro's number. Hirschfelder *et al.*[5] recommend the use of Lennard-Jones potentials for gases of particles with non polar momenta and Stockmayer potentials for gases of polar particles, They give tables of $B(T)$ for different reduced temperatures and different reduced dipolar momenta. In mixtures where both polar and non-polar molecules are present, it is necessary to specify the interaction between polar and non-polar molecules. The force constant describing the potential of interaction between a polar (subscript p) and a non-polar (subscript n) molecule may be obtained from empirical combining laws:

$$\sigma_{n,p} = 0.5(\sigma_n + \sigma_p)\xi^{-1/6}, \tag{2}$$

where σ_p and σ_n are respectively the polar and non-polar widths of the potential wells, the factor ξ being given by

$$\xi = \left[1 + \frac{1}{4}\frac{\alpha_n \mu_p^{*2}}{\sigma_n^3}\sqrt{\frac{\varepsilon_p}{\varepsilon_n}}\right], \tag{3}$$

where

$$\mu^* = \frac{\mu'}{\sqrt{\varepsilon\sigma^3}} \tag{4}$$

μ' being the dipole moment, α_n the polarizability of the non-polar molecule, ε_n and σ_n respectively, the depth and width of the potential well. Table I summarizes the data used for the species considered.

2.3. Transport Properties

The composition and pressure for given temperatures and volumes are first determined using the RAND (RAND for Research and Development is a US non profit independent private institution) method of minimization of the Gibbs free energy of the system[4] and the thermodynamic data.[11–13] The transport properties are calculated according to methods already described in Refs. 5, 14. They are based on the solution of Boltzmann's integro-differential equation using the method of Chapman and Cowling.[15] The calculation of the electrical conductivity is performed to the third approximation, as recommended by Devoto.[16] The thermal conductivity is determined as the sum of four components: the heavy species translational thermal conductivity, the electron translational thermal conductivity, the internal thermal conductivity, all developed to the second approximation, and the reactional conductivity calculated,

Table I. Characteristic Parameters of the Energy Potential of the Chemical Species Considered to Calculate Virial Corrections

Chemical species	Dipole moment (Debyes) (1 Debye = 3.162×10^{-25} $(\mathrm{J\,m^3})^{1/2}$ from[5]	Polarizability ($10^{-30}\,\mathrm{m^3}$) from[6]	Potential width $\sigma(10^{-10}\mathrm{m})$ from[6]	ε/k (Kelvins) (with k as Boltzmann constant) from[6]
CO	0.12	1.95	3.690	91.7
CO_2	0	2.65	3.941	195.2
O_2	0	1.6	3.467	106.7
O	0	0.75 from[7]	1.40 (Van der Waals radius)	–
C	–	1.76 from[8]	1.85 (Van der Waal radius) 4.70 from[9]	5890.67 from[10] 370 from[9]
C_2		2.02[5]	5.27	1380 from[9]
CH_4	0	2.60	3.758	148.6
H	0	–	0.78 (atomic radius)	–
H_2	0	79	2.827	59.7
HO	–	–	0.96 (from ourselves)	–
H_2O	1.84	1.48 from[5]	2.641	809.1
Fe	–	8.4 from[8]	1.24 (atomic radius)	3603 from boiling temperature T_b (with empirical rule $\varepsilon/k = T_b/0.87$)
Ar	0	1.65411 from[8]	3.542	93.3

according to the theory of Butler and Brokaw,[17] to the first approximation. The viscosity, which is that of heavy species, is calculated to the first approximation. The interaction potentials used were found in standard references and are summarized below.

Neutral–neutral interactions are treated as classical potentials, and effective collision integrals are determined from different tabulated functions of potential parameters: Smith and Munn[18] for a Morse potential, Brokaw[19] for a repulsive exponential potential, Monchick[20] for an attractive exponential potential, and Hirschfelder *et al.*[5] for a Lennard–Jones potential and a Stockmayer potential for polar species, with Hirschfelder *et a1.*[5] tables, sometimes used taking into account Eq. (2).

E.g. for the C–C, C–C_2, Ar–C, Ar–C_2, H–C, H–C_2, H_2–C, H_2–C_2, interactions, a Lennard-Jones potential is used and for a collision between polar particles or between a polar particle and a non-polar one such as CO–CO_2, H_2–CO_2, H_2–CO, H–CO_2, H–CO a Stockmayer potential is used. It is worth noting that a Lennard–Jones potential is a particular case, $\mu' = 0$, of the Stockmayer potential. Table II summarizes different collision potentials used. For other neutral–neutral interactions particularly with OH and H, the hard-sphere model has been used with radii reported in Table I.

For ion-neutral interactions two types of interactions must be considered. The interaction between an atom and an ion from a different species, which is purely elastic, is described by a polarization potential. The effective collision integrals are then calculated with the expression given by Kihara *et al.*[21] The polarizability values used are reported in Table I. In

Table II. Neutral-neutral Collision Potentials

Ar	C	H	O	Fe	C_2	CO	CO_2	CH_4	HO	H_2O	O_2	
LJ	LJ	LJ	LJ	LJ	LJ	SM	LJ	LJ	HS	SM	LJ	Ar
	LJ	LJ	LJ	LJ	LJ	SM	LJ	LJ	RS	SM	LJ	C
		LJ	LJ	LJ	LJ	LJ	LJ	LJ	RS	LJ	LJ	H
			LJ	LJ	LJ	LJ	LJ	LJ	RS	SM	LJ	O
				LJ	LJ	LJ	LJ	LJ	RS	LJ	LJ	Fe
					LJ	LJ	LJ	LJ	RS	LJ	LJ	C_2
						SM	SM	SM	RS	SM	SM	CO
							LJ	LJ	RS	SM	SM	CO_2
								LJ	RS	SM	LJ	CH_4
									RS	RS	RS	HO
										SM	LJ	H_2O
											LJ	O_2

RS: hard-sphere, LS: Lennard–Jones potential and SM: Stockmayer potential for a collision between polar particles.

Table III. References of Data of Momentum Transfer Cross-section for Electron–Neutral Interactions

E-neutral	Ar	C	C_2	H	H_2	O	O_2	CH_4	CO	CO_2	HO	H_2O	Fe
From	(23)	(23)	*	(22)	(23)	(23)	(22)	(24)	(24)	(24)	*	(24)	*

*Corresponds to the Kihara's model of polarizability.

the case of a collision between an atom and one of its ions as for Ar/Ar^+, C/C^+, H/H^+, O/O^+ the charge transfer integral is calculated as described in Ref. (22).

Electron–neutral interactions are calculated by integrating, in the case of isotropic diffusion, experimental data of momentum-transfer cross sections, and in other cases by using the Kihara's model of polarizability[21] as reported in Table III. Interactions between charged particles are described by a screened Coulomb potential and collision integrals are calculated from the tables of Mason *et al.*[25]

2.4. Main Mixtures Considered

Table IV summarizes the species considered at room temperature (starting mixture) and those which could appear when temperature increases.

Table IV. Species Considered

Starting species (mole number)	Species appearing at different temperatures
CO (1 mol)	Gaseous species: e, C^+, C^{2+}, O^-, O^{2-}, C^+, CO^+, CO_2^+, C_2^+, O^+, O_2^+, O^{++}, C, CO, CO_2, C_2, C_2O Solid species: C(s)
CH_4 (1 mol)	Gaseous species: e, C^-, C^{2-}, H^-, C^+, CH^+, C_2^+, H^+, H_2^+, H_3^+, C, CH, CH_2, CH_3, CH_4, C_2, C_2H, C_2H_2, C_2H_4, C_2H_6, H, H_2 Solid species: C(s)
CO (0.5 mol) + Fe (0.5 mol)	Gaseous species: e, C^+, C^{2+}, Fe^+, Fe^{++}, O^-, O^{2-}, C^+, CO^+, CO_2^+, C_2^+, O^+, O_2^+, O^{++}, C, CO, CO_2, C_2, C_2O, Fe Solid species: C(s), Fe(s)
CO (0.5 mol) + Ar (0.5 mol)	Gaseous species: e, Ar^+, Ar^{++}, C^+, C^{2+}, O^-, O^{2-}, C^+, CO^+, CO_2^+, C_2^+, O^+, O_2^+, O^{++}, Ar, C, CO, CO_2, C_2, C_2O Solid species: C(s)

3. RESULTS AND DISCUSSIONS

3.1. Main Consequences of Constant Volume

When considering the most simple case, a perfect gas law ($pV = n'RT$), it can be readily seen that, with a constant volume when T increases, p must increase to keep the total number of moles at least constant (assuming no dissociation and no ionization). Thus a constant volume calculation will be characterized by a pressure increase with temperature. To illustrate the consequences of the pressure increase Fig. 1 represent the evolution with temperature of the mole number of the different species which appear when heating one mole of CO.

Figure 1a corresponds to the conventional constant pressure (0.1 MPa) and Fig. lb to c to constant volume for two different initial pressures respectively of 0.1 and 10 MPa. At constant pressure below 1800 K, CO can react to give C(s) + CO_2 but the number of moles of C(s) is very low. CO dissociates at about 6000 K with the formation of O and C. According to the ionization potentials (see Table IV) C^+ ions are the first to show up at higher temperatures. Over about 14,000 K the electron number of mole becomes higher than 1.

At constant volume below 2000–3000 K, depending on the initial pressure, solid carbon is formed but disappears rather fast with the

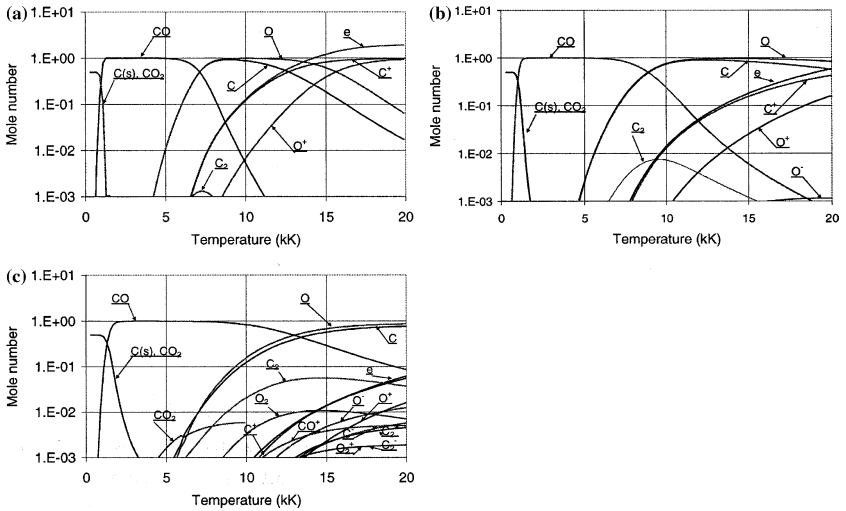

Fig. 1. Evolution with temperature of the mole number of the different species when starting from 1 mol of CO at constant pressure (0.1 MPa) (a) and at constant volume defined at 300 K and two initial pressures respectively of (b) 0.1 MPa, (c) 10 MPa.

Table V. Electron Number of Moles and Densities at 20,000 K

P (MPa)	0.1	1	10
n'_e (number of moles)	0.538	0.194	0.0596
$n_e(m^{-3})$	$1.32 \times 10^{+26}$	$4.78 \times 10^{+25}$	$1.47 \times 10^{+25}$

Starting mixture: 1 mol of CO at constant volume defined at 300 K for three pressures: 0.1 MPa or 1 MPa or 10 MPa.

formation of CO. As it can be seen the initial pressure increase delays the dissociation of CO (its mole number is 10^{-1} at 8000 K at constant pressure and at constant volume this mole number is reached at 11,500 K when the initial pressure is 0.1 MPa and 18,000 K for an initial pressure of 10 MPa). At constant volume, at 10 MPa when CO dissociation starts, carbon is replaced by C_2^+, C^+ and C_2^-. In both cases ($p_{init} = 0.1$ or 10 MPa) ionization is mainly due to the carbon. It can also be seen that at 10 MPa O_2 can be formed between 10,000 and over 20,000 K, however in small quantities $n'_{O_2} < 10^{-2}$. Of course when the initial pressure increases for the same temperature, the electron number of moles as well as their densities decrease (see Table V), with a corresponding increase of neutral species densities.

The evolution with temperature at constant pressure of CH_4 is shown in Fig. 2a and at constant volume for an initial pressure of 0.1 MPa at 300 K in Fig. 2b. Compared to CO in the low temperature range ($T <$ 1000 K) the decomposition of CH_4 induces the formation of solid carbon which sublimes at about 4000 K. The resulting H_2 starts to dissociate at about 3500 K at constant pressure (see Fig. 2a) and at 4800 K at constant volume for an initial pressure of 0.1 MPa (see Fig. 2b). This dissociation is much slower at constant volume. At constant pressure (see Fig. 2b) H atom mole number is constant up to 13,500 K. Below 9000 K, ionization is due to both of C^+ and H^+. The mixture is fully ionized only over 17,000 K.

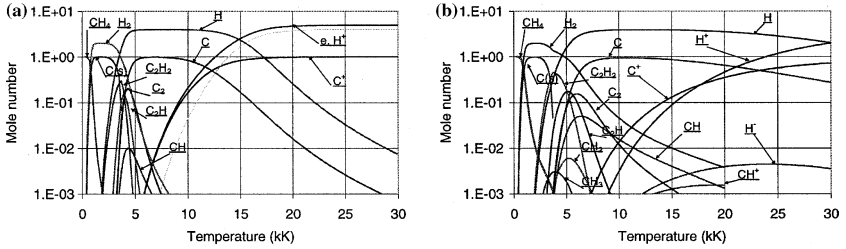

Fig. 2. Evolution with temperature of the mole number of the different species when starting from 1 mol of CH_4. (a) At constant pressure 0.1 MPa; (b) constant volume with an initial pressure 0.1 MPa at 300 K. Graphite is labeled C(s).

At constant volume (see Fig. 2b) the same phenomena are observed but as H_2 dissociation is slower, H is hardly ionized below 17,000 K and electrons are mainly due to C^+. Over that temperature H^+ take over.

The net result for the pressure is shown in Fig. 3a where different mixtures at constant volume are considered starting from one mole (initial condition: $T = 300\,\text{K}$, $p = 0.1\,\text{MPa}$). As it could be expected, CH_4 results in the highest pressure: the total dissociation of CH_4 produces 5 moles of atoms and its total ionization 5 moles of ions and 5 moles of electrons. Pure CO over 8000 K produces more atoms and their ions than the mixtures of 0.5 moles of CO with 0.5 mol of either Ar or Fe. The CO–Fe mixture with the low ionization potential of Fe creating Fe^+ and then Fe^{++} results in a higher pressure than the CO–Ar mixture where at 20,000 K the formation of Ar^{++} is hardly starting.

The second virial correction when pressure increases is only noticeable for $T \leq 20,000\,\text{K}$ for an initial pressure higher than 0.1 MPa. It has been represented for CO in Fig. 3b through the compressibility factor $Z = pV/n'RT$. When $Z = 1$ the first virial correction is negligible. It becomes really important only for an initial pressure of 10 MPa. The curve behavior is in good agreement with similar curves presented by Hirschfelder *et al.*[5] At the Boyle temperature T_{Boyle} intermolecular attractive and repulsive effects are balanced ($B(T) = 0$). For most gases, experiment shows that the ratio of the Boyle temperature to the critical temperature is consistently about 2.75 (except for He) and for CO T_{Boyle} is about 1000 K. In Fig. 3b, Boyle temperature corresponds to the intersection of the curves with the horizontal of the compressibility factor equal to one.

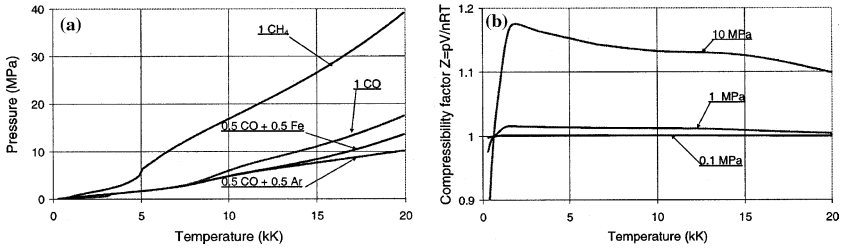

Fig. 3. (a) Evolution of the pressure at constant volume of 1 mol of CH_4, 1 mol of CO, 0.5 mol of CO plus 0.5 mol of Fe, 0.5 mol of CO plus 0.5 mol of Ar (constant volume defined at 300 K and an initial pressure of 0.1 MPa); (b) evolution of the compressibility factor $Z = pV/n'RT$ (n' total mole number) at constant volume when starting from 1 mol of CO at three different initial pressures (a) 0.1 MPa, (b) 1 MPa and (c) 10 MPa.

3.2. Electrical Conductivity

The electrical conductivity σ_e is proportional to the electron density n_e[26] and inversely proportional to collision cross sections of electrons with different species σ_{ei} multiplied by the species (or target) densities n_i. (see Eq. 5).

$$\sigma_e = \frac{n_e e^2}{\sqrt{2\pi T m_e} \sum_i n_i \sigma_{ei}}. \tag{5}$$

Figure 4a represents σ_e at constant pressure (0.1 MPa) and constant volume (calculated at 300 K, 0.1 MPa). In both cases, below 15,000 K, n_e depends mainly on C^+ as shown in Fig. 4b and c.

Below 15,000 K at constant pressure and constant volume σ_e follows the drastic increase of n_e with temperature which is larger at constant pressure than at constant volume. Over 15,000 K at constant pressure n_e does not vary very much with temperature and ions become the most important species with collision cross sections with electrons higher than those between electrons and neutrals. Thus the temperature evolution of σ_e with T becomes slower than at constant volume. At constant volume

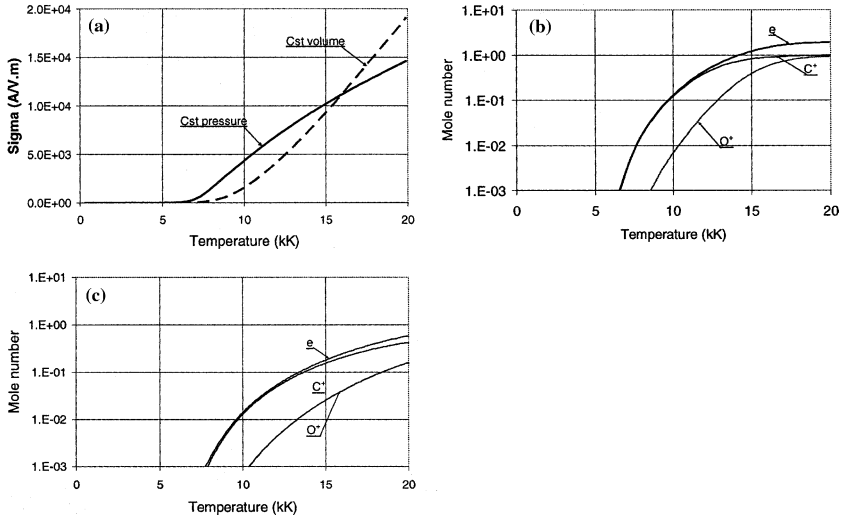

Fig. 4. Evolution with temperature for 1 mol of CO of (a) the electrical conductivities, respectively, at constant pressure ($p = 0.1$ MPa) and constant volume (calculated at 300 K and an initial pressure of 0.1 MPa); (b) the number of moles of electrons, C^+ and O^+ species at constant pressure $p = 0.1$ MPa; (c) the number of moles of electrons, C^+ and O^+ species at constant volume (calculated at 300 K and an initial pressure of 0.1 MPa).

Table VI. Ionization Energy for Different Atomic Species From[11]

Species	Fe	Fe^+	Fe^{++}	Ar	Ar^+	Ar^{++}	C
Ionisation energy (kJ/mol)	759.3	1561	2957	1520	4185	8113	1086.2
Species	C^+	C^{++}	H	O	O^+	$C_2 \Rightarrow C_2^+$	$C_2 \Rightarrow C_2^-$
Ionisation energy (kJ/mol)	3438.2	8058.2	1312	1313.9	5202.1	1992	−342

(see Fig. 1a), in spite of the fact that ionization is delayed when pressure increases, and electron density decreases (see Table V and compare Fig. 4b and c) σ_e increases because more neutral species are present over 15,000 K, with a much lower collision cross section with electrons (see Eq. (5)). Of course the addition of Ar to CO changes little about σ_e (n_e is still mainly due to C^+) (see Fig. 5a). When adding Fe to CO a difference (see Fig. 5b) can be observed, especially at temperatures below 15,000 K, due to the lower ionization potential of Fe (see Table VI). With CH_4 (see Fig. 5a) as shown in Fig. 2 the pressure increases by far more drastically than that of CO and less ionized species exist at the same temperature (2% at 10,000 K against 12% for CO, resulting in an electrical conductivity lower than that of CO (see Fig. 5a).

3.3. Viscosity

In the frame of the simple kinetic theory, the viscosity μ is independent of pressure and it varies as

$$\mu = \frac{\sqrt{mkT}}{\sigma_{i,j}\overline{\Omega}_{i,j}^{l,s}}, \tag{6}$$

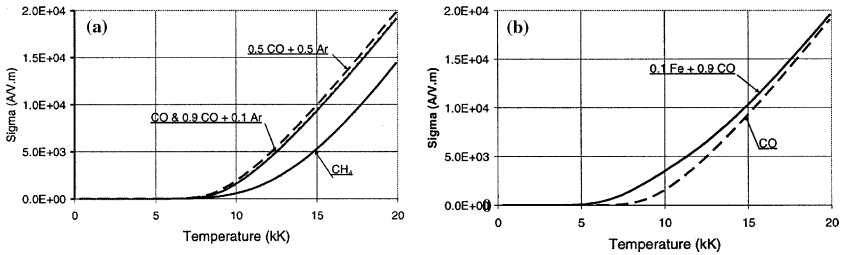

Fig. 5. Evolution with temperature at constant volume (initial pressure = 0.1 MPa) of the electrical conductivity of (a) CO, 0.9 CO + 0.1 Ar, CH_4, 0.5 CO + 0.5 Ar, (b) 0.9 CO + 0.1 Fe and CO.

where σ_{ij} is the collision cross-section of particles, considered to be hard spheres, and $\overline{\Omega}_{i,j}^{l,s}$ the corresponding reduced collision integral (l and s depending on the approximation degrees).

While this expression is not accurate in a gas mixture or plasma, it gives nevertheless the underlying trends:[14]

- the square root of the mass explains partly why the viscosity of CO is higher than that of CH_4.
- below the dissociation the viscosities of products resulting from dissociation are lower than those of the initial molecules.
- As the cross sections of products resulting from dissociation are lower than those of the initial molecules, after dissociation.

When the electron mole number is between 1 and 30%, depending on the gas and its pressure, μ decreases due to the long range interactions of charged particles. Figure 6a shows the evolution of viscosity with temperature both at constant volume (initial pressure of 0.1 MPa) and pressure for CO and Fig. 6b for CH_4. With CO at constant pressure, when the dissociation of CO at about 5800 K (see Fig. la) starts, as the collision integrals of O–O and C–C are smaller than that of CO–CO there is a rapid increase of μ up to about 9000 K. This temperature corresponds to a molar fraction x_e of charged species of about 0.03. For higher temperatures with the increase of n_e, μ decreases regularly up to the end of first ionization around 17,000 K. At constant volume due to the significant pressure increase (see Fig. 3a), dissociation of CO is shifted to about 7000 K (see Fig. la) and the maximum of μ is reached at 14,000 K where $x_e = 0.08$. Of course as first ionization is far from complete at 20,000 K, μ decreases more slowly than at constant pressure. With the pressure increase and the

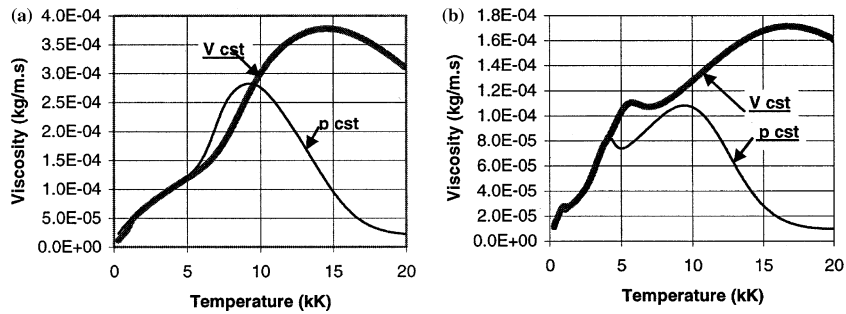

Fig. 6. Evolution with temperature of the viscosities respectively, at constant pressure of 0.1 MPa and constant volume (calculated at 300 K and an initial pressure of 0.1 MPa) of: (a) CO, (b) CH_4.

shift of ionization to higher temperatures μ at constant volume is larger than at constant pressure.

With CH_4 a similar behavior is observed. At constant pressure the first maximum observed at about 4200 K corresponds to the sublimation of the carbon with the formation of C_2H from C_2H_2 (see Fig. 2a). At constant pressure μ starts to decrease at about 9500 K corresponding to $x_e \sim 0.01$. While at constant volume the decrease is observed only over 16,500 K when $x_e > 0.015$. Below 1000–1500 K the dissociation of CH_4 induces a slight variation of μ.

When comparing CO and CH_4 the maximum value of μ obtained with CH_4 is smaller than that determined with CO, due to the lower mass of CH_4.

Figure 7 represents the temperature evolution of the viscosity of a mixture of CO–Fe (0.5 mol each). With the low ionization potential of Fe (see Table IV), at constant pressure $x_e = 0.0756$ at 7500 K and thus the viscosity decreases sooner than that of pure CO. Its peak value is also lower due to the presence of only 0.5 mol of CO. At constant volume μ starts to decrease at 13,000 K ($x_e = 0.116$), compared with 7500 K at constant pressure, and its decrease is much slower than that observed with pure CO (see Fig. 6a).

3.4. Thermal Conductivity

Thermal conductivity K of plasmas is the sum of the translational thermal conductivity of heavy species K_h and electrons K_e, the internal

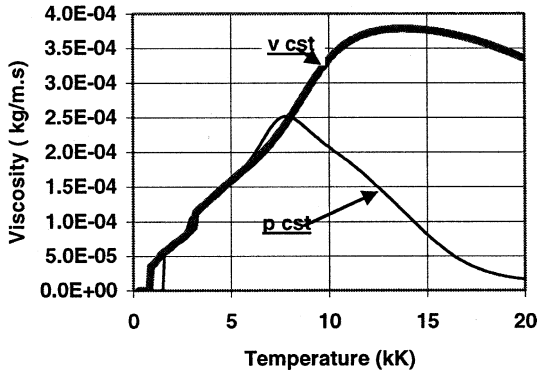

Fig. 7. Evolution with temperature of the viscosity of a mixture CO–Fe (0.5 mol each) at constant pressure (0.1 MPa) and constant volume (calculated at 298 K and initial pressure of 0.1 MPa).

thermal conductivity K_{int} (almost negligible) and the reaction thermal conductivity K_r, due to dissociation and ionization phenomena. It depends strongly on the reaction terms (dissociation and ionization). When the pressure increases[14] the dissociation and ionization are delayed to higher temperatures and dissociation peaks are lowered while the ionization ones are increased. Figure 8 shows the corresponding results for CH_4 and CO.

For CH_4 at constant pressure of 0.1 MPa the first peak at about 4000 K is in good agreement with the dissociation of H_2 (see Fig. 2b) while the second, slightly over 15,000 K corresponds to the maximum ionization of H[27]. Over 15,000 K ionization is completed and K_R decreases, however the total thermal conductivity K_t decreases very slowly, the translational thermal conductivity of electrons taking over the K_R decrease only for $T > 18,500$ K (see Fig. 9a) where K_t increases again. For the constant volume, dissociation of H_2 is shifted slightly over 5000 K and at 20,000 K ionization of carbon and hydrogen is not completed, thus the ionization peak is not reached (see Fig. 9b).

For CO at constant pressure, dissociation occurs at about 7000 K (see Fig. 1a), while at constant volume ($p_{init} = 0.1$ MPa) it is shifted to about 8500 K (see Fig. 1a) the two peaks observed in Fig. 8b corresponding to these temperatures. Ionization is due first to C^+ and then to O^+ and the electron density keeps increasing. The electron translational thermal conductivity increases accordingly (see Fig. 9b); thus there is no marked ionization peak in the temperature range considered both at constant pressure and constant volume. When comparing CH_4 and CO the thermal conductivity of the former is higher than that of the latter due to the more efficient heat transfer of hydrogen.[28]

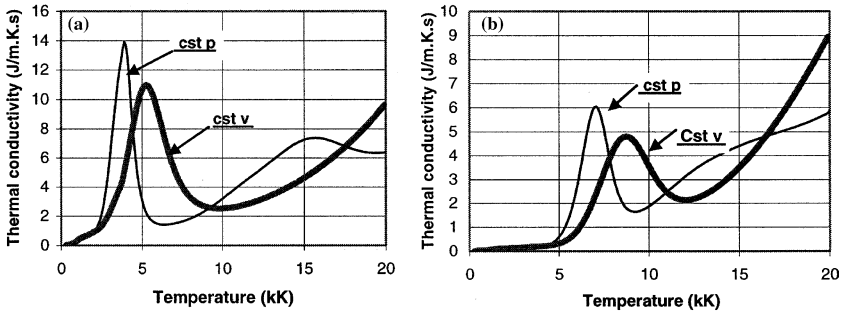

Fig. 8. Evolution with temperature of the thermal conductivities at constant volume (calculated at 300 K and an initial pressure of 0.1 MPa) and constant pressure (0.1 MPa), respectively, of (a) CH_4, (b) CO.

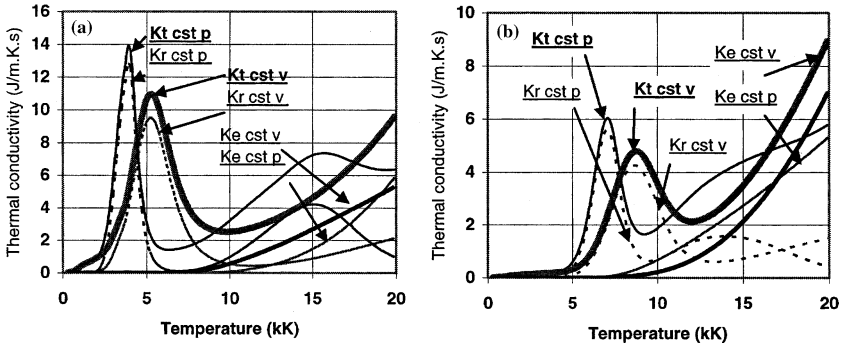

Fig. 9. Reaction, total and translational (electrons) thermal conductivities at constant pressure (0.1 MPa) at constant volume (calculated at 300 K and initial pressure of $p = 0.1$ MPa) of (a) CH_4, (b) CO.

With a CO–Fe mixture (0.5 mol each) the dissociation peaks are observed at the same temperature as those of pure CO. They are of course lower than those of pure CO (only 0.5 mol). With the ionization of Fe at lower temperature, the electron translational thermal conductivity is higher than that of pure CO (Fig. 10a and b) at the same temperature and no ionization peak is observed any more even at constant pressure.

4. CONCLUSIONS

The main effects when calculating the composition at constant volume is the drastic increase of pressure with the temperature (up to 40 MPa at 20,000 K with CH_4 when starting at 0.1 MPa at 300 K). As a result disso-

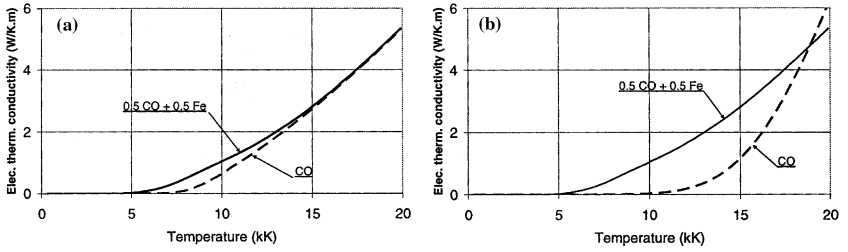

Fig. 10. (a) Electron thermal conductivities at constant pressure ($p = 0.1$ MPa) of CO and the mixture CO–Fe (50%, 50%), respectively; (b) electron thermal conductivities at constant volume (calculated at 300 K and an initial pressure of $p = 0.1$ MPa) of CO and the mixture CO–Fe (50%, 50%), respectively.

ciation and ionization are shifted to higher temperatures. When pressure increases, the electron density is lowered (higher ionization temperatures) with a correspondingly higher density of neutrals. As the electrical conductivity is proportional to n_e and inversely proportional to the product of the target species density n_i, and the collision cross section of electrons with target species (σ_{ei}), the drastic reduction of σ_{ei} when i corresponds to neutral species and not to ionized ones induces an increase of the electrical conductivity when pressure increases, in spite of the decrease of n_e. Thus at constant volume as soon as $T > 15,000$ K for the considered mixtures (CH_4, CO, 0.9 CO + 0.1 Ar, 0.5 CO + 0.5 Ar, 0.9 CO + 0.1 Fe) the electrical conductivity is higher than that obtained at a constant pressure of 0.1 MPa. At constant volume the viscosity is drastically increased at temperatures over 10,000 K compared to the viscosity at constant pressure. This increase is due to the fact that charged species appear at higher temperatures when pressure increases. For thermal conductivity K_t at constant volume, compared to constant atmospheric pressure, the dissociation and ionization peaks are shifted to higher temperatures. At constant pressure for CH_4 the ionization peak is observed at 15,000 K, but as n_e still increases with the formation of ions, the increase of electron translational thermal conductivity becomes more important than the peak decrease, and over 18,500 K, K_t increases again. For CO at atmospheric pressure the ionization peak is completely overcome by the electron translational thermal conductivity. At constant volume the ionization phenomena are shifted to higher temperatures and at 20,000 K no ionization peak is reached.

REFERENCES

1. D. Neuschütz, *J. High Temp. Mater. Process*. **2**, 261 (1998).
2. D. Neuschütz, *J. High Temp. Mater. Process*. **5**(1), 127 (2000).
3. P. Fauchais, M. F. Elchinger, and J. Aubreton, *J. High Temp. Mater. Process*. **5**(1), 21 (2000).
4. W. B. White, S. M. Johnson, and G. B. et Dantzig, *J. Chem. Phys*. **28**(5), 751 (1958).
5. J. O. Hirschfelder, C. F. Curtiss, and B. R. Byron, *Molecular Theory of Gases and Liquids*. (Pub.) John Wiley and Sons, second printing, New York 1964, pp. 151, 163, 209–219, 949–950, 988, 1147–1151, 1114–1115.
6. R. C. Reid, J. M. Prausnitz, and B. E. Poling, *The Properties of Gases & Liquids*. (Pub.) McGraw-Hill Book Company, 4th edn, New York 1987, pp. 658–664.
7. C. W. Allen, *Astrophysical Quantities*, (Pub.) Athlone Press, 1964.
8. *Handbook of Chemistry and Physics*, 67th Edition, (Pub.) CRC-Press, 1997–1998.
9. C. Benjamin, Calculation of Transport Properties and Study of the Switching Efficiency of the Mixture SF6-CF4 or C2F6 and SF6–Cu Vapor (in French), PhD thesis, University Paul Sabatier, Toulouse III, No. 1997, 28/03/1995.
10. Z. Koalaga, Contribution to the Experimental and Theoretical Study of Laminated Plasma Produced by d.c. Arcs (in French), PhD thesis, Clermont-Ferrand University, France, 1991.

11. L.V. Gurvich et al., *Thermodynamic Properties of Individual Substances*, (Pub.) Hemisphere, NY 4th 1996.
12. M. Chase et al., *JANAF Thermochem*. Tables, 3rd edn. *J. Phys. Chem*. Ref. Data, 1985. 14 (Supp. 1).
13. I. Barin, *Thermochemical Data of Pure Substances*, (Pub) Springer Verlag, Berlin 1993.
14. B. Pateyron, M. F. Elchinger, G. Delluc, and P. Fauchais, *Plasma Chem. Plasma Processing* **12**(4), 421 1992.
15. S. Chapman and T. Cowling, *The Mathematical Theory of Non Uniform Gases*. Cambridge University Press, New York 1952.
16. R. S. Devoto, *Phys. Fluids* **16**, 616 (1973).
17. J. N. Butler and R. S. Brokaw, *J. Chem. Phys*. **26**, 1636 (1957).
18. F. J. Smith and R. J. Munn, *J. Chem. Phys*. **41**, 3560 (1964).
19. R. S. Brokaw, *Phys. Fluids* **8**, 944 (1961).
20. L. Moonchick, *Phys. Fluids* **2**, 695 (1959).
21. T. Kihara, M. H. Taylor, and J. O. Hirschfelder, *Phys. Fluids* **3**(5), 715 (1960).
22. J. Aubreton, Study of the Thermodynamic and Transport Properties in Equilibrium and Non Equilibrium Thermal Plasmas: Application to Ar-H2 et Ar-O2 Mixtures (in French), State thesis, Limoges University, France, 1985.
23. Y. Itikawa, *Data Nucl. Data Tables* **14**, 1 (1974).
24. Y. Itikawa, *Data Nucl. Data Tables* **21**, 69 (1978).
25. E. A. Mason, R. J. Munn, and F. J. Smith, *Phys. Fluids*, **l0**(8), 1827 (1967).
26. J. W. Gallagher, JILA Data Center, Campus Box 440, Colorado University, Boulder, Colorado 80309, USA. (Also ftp://jila.colorado.edu/collision_data/electron.txt)
27. M. F. Elchinger, B. Pateyron, G. Delluc, and P. Fauchais, *J. de Physique colloque* C5, **51**(185), C5.3 (1990).
28. M. I. Boulos, P. Fauchais, and E. Pfender, *Thermal Plasmas vol. 1* (Pub.) Plenum Press NY 1994.